Supplementary material

1. Effects of craniotomies on E-field distribution in tDCS

To assess the possible effects of a craniotomy on the E-field distribution induced by tDCS, we used a template head model based on data from Colin27's template (https://www.mcgill.ca/bic/software/tools-data-analysis/anatomical-mri/atlases/colin-27). The methods used to create the head model are described in (Miranda et al, 2013). Electrodes representing Neuroelectrics' NG PiStim were added to the head model in a similar manner to what was done in the head models created for this study. The tissue conductivities were also set to the same values used in this study: 0.3 S/m for the skin, 0.008 S/m for the skull, 1.79 S/m for the CSF (including the ventricles), 0.4 S/m for the grey-matter (GM) and 0.15 S/m for the white-matter (WM). The gel under each electrode was modeled with a conductivity of 4.0 S/m.

Craniotomies were modeled as a central hole filled with CSF (representing an "acute-phase" lesion) with a radius of 1.0, 2.5 and 5.0 mm surrounded by a gap between the bone flap and the rest of the skull (radius of bone flap of 20 mm, distance between flap and skull of 2.0 mm). Since many of the targets in this study were in the temporal region of the brain, we place the central hole directly under electrode T7 in the template head model. The model of the craniotomy is represented *in figure 1a*. All calculations were performed in Comsol 5.3a (www.comsol.com).

To assess safety, we calculated the E-field distribution with a montage employing T7 as an anode (current of 1.884 mA, the maximum allowed per electrode in this study) and Cz as the cathode. The presence of the burr hole increased the E-field peak value from 1.22 V/m to 4.25 V/m (2.5 mm radius central hole). The increase with other hole sizes was smaller (see figure 1b). There was also an increase under the gap between the bone flap and the skull, but the peak value there was smaller.

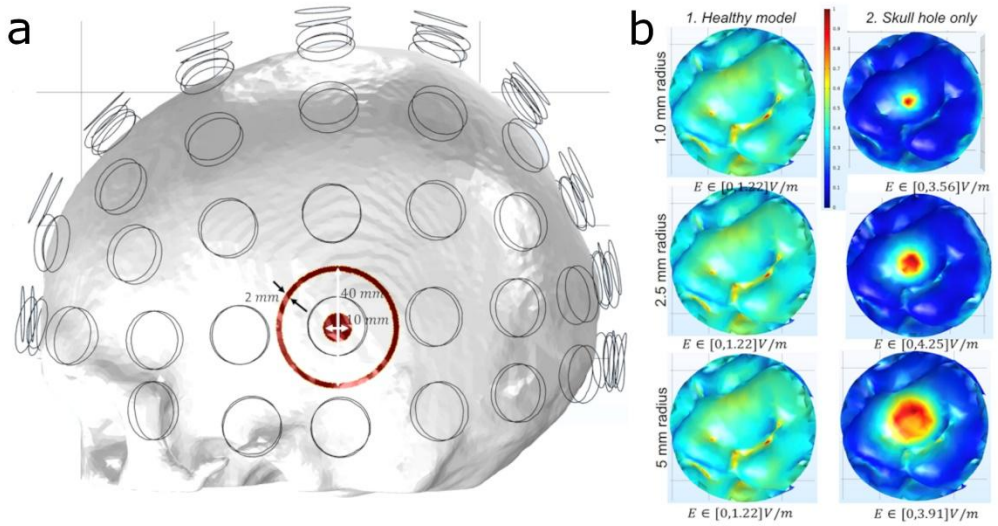

Figure 1: Impact of a craniotomy of the magnitude of the E-field induced with tDCS. a) Representation of the craniotomy consisting of a central whole inside a bone flap that is located at a 2 mm gap from the skull; b) E-field magnitude directly under the central hole for the healthy model (left column) and the models with central holes with increasing radius.

2. Effects of craniotomies on total injected current in optimized montage

In order to test the influence of craniotomies in the results of montage optimization, we used the same head model as before, only now with the craniotomy located under electrode C3 (see figure 2). For simplicity we modeled the craniotomy in this case as a 1.0 cm radius cylindrical region with a conductivity equal to that of the CSF. The target for the optimization was defined by intersecting a cylinder with a radius of 1 cm to the cortical surface. We used three targets in this case: one under C3 (directly under the skull lesion), one under P3 and another one under T7. The target E_n field was set to +0.25 V/m in this cortical region and 0.0 V/m in the remaining areas. Weights for the optimization were set to 10 for the target region and 2 for the remaining areas. We ran optimizations with a maximum of 2 and 6 channels, and with current constraints set to 2.0 mA max per electrode and 4.0 mA max total injected current (double of what was used in the protocol followed for the patients, reported in the main manuscript). The optimizations conducted with the craniotomy were compared with optimizations conducted for an intact skull.

For the optimizations conducted with the target under C3, the maximum value of the E_n-field were similar across models (0.23-0.29 V/m), however, the total injected current was much smaller in the model with the skull hole than in the model with the intact skull (42-52% reduction). Regarding the average E_n-field at the target, it was higher in the model with the skull hole in the two-channel montage (49% increase, relative to the model with the intact skull). In the six-channel optimization, this increase was much smaller: 0.44%. Table 1 presents a summary of the total injected current and the average E_n-field at the target for all the montages considered in this study.

The distribution of the E_n-field (see figure 3) was also much more focalized at the target for the skull hole model in the 2-channel montage (first row of figure 3). But the impact of the skull hole in the 6-channel montage was much smaller (second row of figure 3).

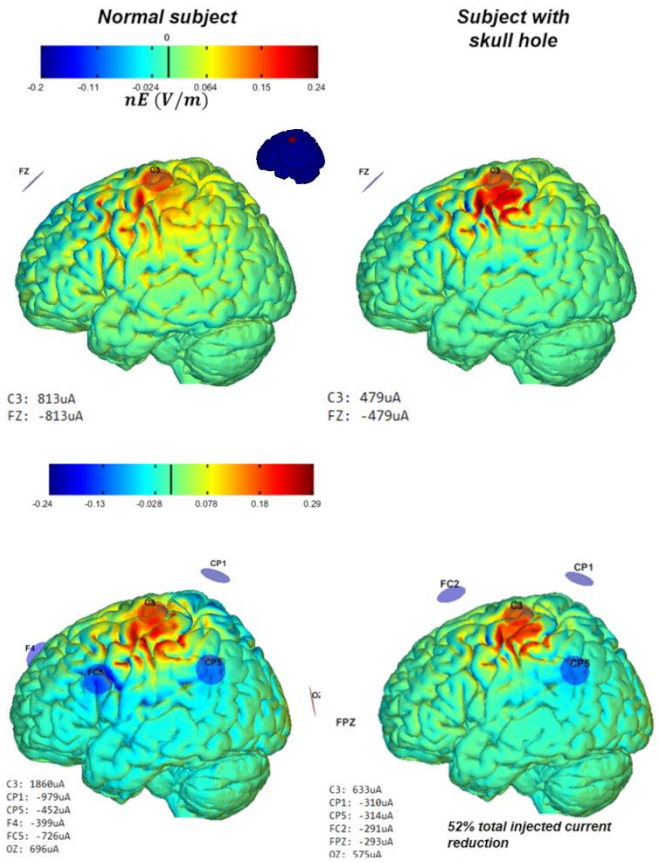

Figure 2: Impact of a skull lesion in a montage optimization for a target directly under the hole. Left column shows the results with the intact skull, whereas the right column shows the results with the skull hole. The top/bottom rows show the results of the optimization constrained with a maximum of 2/6 channels. The inset in the top-left figure shows the target used in the optimization.

Target	Number of channels	Intact skull		Skull hole		Relative difference	
		$\langle E_n \rangle$ (V/m)	Total inj. I (mA)	$\langle E_n \rangle$ (V/m)	Total inj. I (mA)	$\langle E_n \rangle$	Total inj. I
C3	2	0,027	0,813	0,040	0,479	49,0	-41,1
	6	0,048	2,556	0,049	1,208	0,4	-52,7
P3	2	0,067	1,346	0,067	1,327	-0,4	-1,4
	6	0,077	2,417	0,078	2,398	0,2	-0,8
T7	2	0,016	0,732	0,016	0,732	-0,2	0,0
	6	0,029	2,747	0,029	2,747	-0,1	0,0

Table I: Average E_n at the target (V/m) and total injected current for all the montages and skull models in this study. The last two columns show the differences between the skull hole values and the intact skull one as a percentage of the intact skull values.

For the optimizations conducted for the targets located over P3 and T7, the presence of the skull hole under C3 affected much less the results. This is shown in table 1, where the maximum relative difference between the injected currents is of only -1.4% and the maximum relative difference in the average E_n-field is only -0.8%. Even the positions and currents of each individual electrodes are very similar, as can be seen in figures 4 and 5 which show the distribution of the component of the E_n-field for the

optimizations conducted with the targets under P3 and T7, respectively. As expected, the distribution of the E_n-field is almost unchanged with the presence of the skull hole.

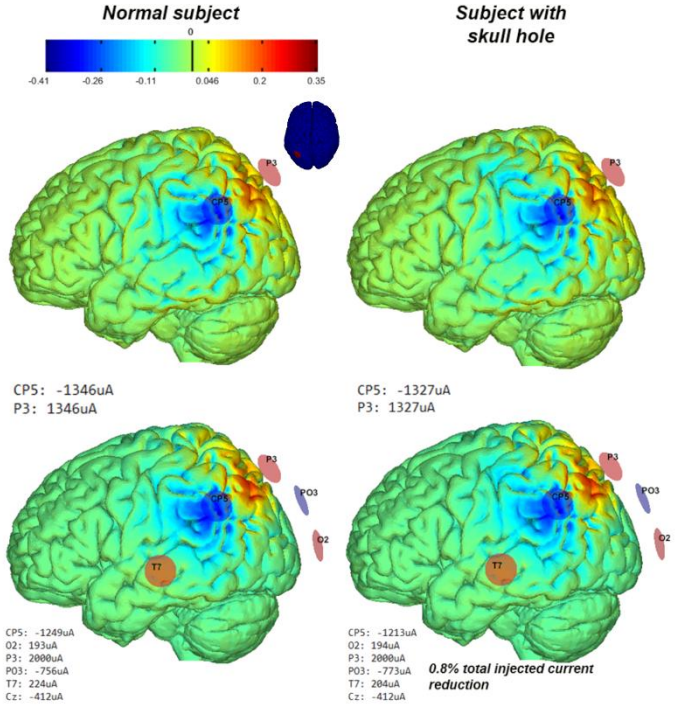

Figure 3: Impact of a skull lesion in a montage optimization for a target under electrode P3. Left column shows the results with the intact skull, whereas the right column shows the results with the skull hole. The top/bottom rows show the results of the optimization constrained with a maximum of 2/6 channels. The inset in the top-left figure shows the target used in the optimization.

3. Discussion

The results presented here show that the presence of skull regions with higher conductivity can influence greatly the E-field distribution as expected. The observed increase in E-field is not, however, enough to reach peak values near the threshold for lesion generation according to animal models: 23 V/m for 60 minutes tDCS protocols and 61 V/m for 20 minutes protocols (Bikson et al, 2016). Furthermore, if correctly segmented and represented in the head model, the montage optimization algorithms adjusts the currents and electrode positions to maintain a similar average E_n on target.

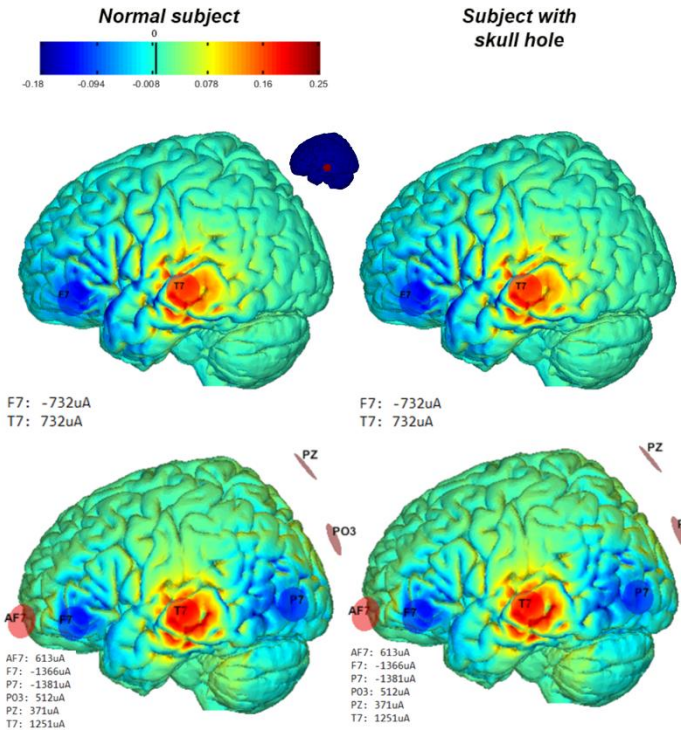

Figure 4: Impact of a skull lesion in a montage optimization for a target under electrode T7. Left column shows the results with the intact skull, whereas the right column shows the results with the skull hole. The top/bottom rows show the results of the optimization constrained with a maximum of 2/6 channels. The inset in the top-left figure shows the target used in the optimization.

4. References

[1] Miranda, P.C., Mekonnen, A., Salvador, R., Ruffini, G., 2013. The electric field in the cortex during transcranial current stimulation. Neuroimage 70, 45–58. https://doi.org/10.1016/j.neuroimage.2012.12.034

[2] Bikson, M., Grossman, P., Thomas, C., Zannou, A.L., Jiang, J., Adnan, T., Mourdoukoutas, A.P., Kronberg, G., Truong, D., Boggio, P., Brunoni, A.R., Charvet, L., Fregni, F., Fritsch, B., Gillick, B., Hamilton, R.H., Hampstead, B.M., Jankord, R., Kirton, A., Knotkova, H., Liebetanz, D., Liu, A., Loo, C., Nitsche, M.A., Reis, J., Richardson, J.D., Rotenberg, A., Turkeltaub, P.E., Woods, A.J., 2016. Safety of Transcranial Direct Current Stimulation: Evidence Based Update 2016. Brain Stimul 9, 641–661. https://doi.org/10.1016/j.brs.2016.06.004